

**A two-stage framework for short-term wind power forecasting using different
feature-learning models**

Jiancheng Qin

School of Computer Science and Technology, Harbin Institute of Technology, Heilongjiang
Province, China, 150000, 1170300519@stu.hit.edu.cn

Jin Yang

School of Computer Science and Technology, Harbin Institute of Technology, Heilongjiang
Province, China, 150000, 1170801219@stu.hit.edu.cn

Ying Chen*

Department of Management Science and Engineering, School of Management, Harbin
Institute of Technology, Heilongjiang Province, China, 150000, yingchen@hit.edu.cn

Qiang Ye

Department of Management Science and Engineering, School of Management, Harbin
Institute of Technology, Heilongjiang Province, China, 150000, yeqiang@hit.edu.cn

*Corresponding author: Phone number: (+86)-451-86414019, Email: yingchen@hit.edu.cn

Department of Economics and Trade, School of Management, Harbin Institute of Technology,
Heilongjiang Province, China, 150000.

Abstract

With the growing dependence on wind power generation, improving the accuracy of short-term forecasting has become increasingly important for ensuring continued economical and reliable system operations. In the wind power forecasting field, ensemble-based forecasting models have been studied extensively; however, few of them considered learning the features from both historical wind data and NWP data. In addition, the exploration of the multiple-input and multiple-output learning structures is lacking in the wind power forecasting literature. Therefore, this study exploits the NWP and historical wind data as input and proposes a two-stage forecasting framework on the shelf of moving window algorithm. Specifically, at the first stage, four forecasting models are constructed with deep neural networks considering the multiple-input and multiple-output structures; at the second stage, an ensemble model is developed using ridge regression method for reducing the extrapolation error. The experiments are conducted on three existing wind farms for examining the 2-h ahead forecasting point. The results demonstrate that 1) the single-input-multiple-output (SIMO) structure leads to a better forecasting accuracy than the other three; 2) ridge regression method results in a better ensemble model that is able to further improve the forecasting accuracy, than the other machine learning methods; 3) the proposed two-stage forecasting framework is likely to generate more accurate and stable results than the other existing algorithms.

Keywords: wind power forecasting, deep neural networks, ensemble learning, extrapolation

1. Introduction

Renewable energy has become a primary focus of academic research and driven changes in power industries. Wind energy is considered a very promising source of such energy [1]. Thus far, China has deployed the largest wind-power capacity (188,390 MW) in the world [2]. The integration of wind power into the power market reduces pollution caused by traditional energy resources (e.g., coal and oil). However, the intermittent and dynamic nature of wind energy adds risk to economical and reliable operations [3]. According to the intraday power market exchange in China, each wind farm is supposed to submit a short-term wind power forecasting (WPF) results every 15 min to a scheduling center, where a composite forecast is built concerning the next 15 min to 4 h. In general, the schedule center selects one time point

within the future 4 h to evaluate the forecasting accuracy. According to the survey, most provinces select a point 2-h ahead; hence, in this paper, we use this time point to examine the performance of our proposed model. For a short-term WPF, existing models can generally be classified into three groups [4]: physical models based on numerical weather prediction (NWP), statistical models based on data-driven intelligent algorithms, and hybrid physical and statistical models.

NWP models simulating the physics of the atmosphere using laws and boundary conditions, have been widely used in the literature [5-11]. However, the direct adoption of NWP models for WPF faces various challenges, such as those of spatial and temporal resolution and accuracy. Compared to NWP models, statistical models, such as autoregressive moving average (ARMA) methods [12, 13], autoregressive integrated moving average (ARIMA) methods [14], Kalman filter [15] and deep neural networks [16-18], use historical data for training, and usually outperform NWP models for short-term WPF. In terms of the hybrid models, they use the historical wind power data and NWP data as input to build the forecasting model. Because of using more input information than the others, such models theoretically lead to better forecasting accuracy as long as they are well developed. For example, Wu et al. [19] used convolutional neural networks (CNN), long short-term memory (LSTM) networks and recurrent neural networks to extract the features from the hybrid data for the development of a 4-h-ahead WPF model; Liu et al. [20] decomposed the hybrid data using wavelet packet and then made use of CNN and LSTM to forecast 10-, 20-, and 30-min-ahead wind speed. However, all the aforementioned researches only use a single model to forecast the all scenarios.

Recently, some researches pay attention to using the ensemble model for improving the forecasting accuracy. As commented by Freedman et al. [21], ensemble models may produce more accurate forecasting results than any of a single model. Briefly, the architecture of an ensemble method builds several models at the first stage and then combines the results from the first stage with an ensemble algorithm at the second stage. For example, Feng et al. [22] exploited several machine learning techniques to build the forecasting models and then integrated the results with an algorithm to further improve the forecasting accuracy; Wang et al. [23] utilized CNN to extract features from each decomposed raw wind power data by

wavelet transform, and then output the forecasting results with an ensemble method; Hao and Tian [24] proposed a two-stage WPF module with a novel nonlinear ensemble method at the second stage to integrate all the components and forecast error values. More related researches could be found in [25-27].

In the ensemble-based researches, some ones only used the historical wind data as input such as [23-27]; by contrast, Feng et al. [22] utilized the NWP data as input to forecast the 1-h-ahead wind speed. Considering the success of the hybrid data (NWP and historical wind data) in the literature, we prefer to use such mixed data to develop the forecasting model. However, NWP and historical wind data are generated by different mechanisms; hence, the internal patterns of different types of data are different. Even though the combination of CNN and LSTM networks has shown distinguished performance in [19] and [20], these researches do not consider the ensemble methods; more importantly, these researches combine and enter the different types of data into the model directly without analyzing whether such a direct combination would cause positive or negative effects on the forecasting accuracy. In addition, for the WPF related researches, the output is always just a single output. In the literature, the structure with multiple outputs has been studied in the deep learning area. As described in Xu et al. [28], multiple-output learning is to simultaneously predict multiple outputs given an input. In addition, Zhao et al. [29] commented that adding an auxiliary output may help gradient pass down to lower layers and make low-level features more accurate so that the over-fitting issue might be prevented. Hence, we further consider adding a wind speed forecasting result as an auxiliary output to investigate whether this structure is likely to improve the forecasting accuracy of wind power. Lastly, in the ensemble-based researches, e.g., [22] and [23-27], machine learning algorithms are usually used to blend the results from the first stage; however, these researches do not consider the usage of the ridge regression (RR) method, which is likely to reduce the extrapolation error [30]. In statistics, when examining the model with the data that is over the original range, the extrapolation of the model would occur [31].

To bridge the gap discussed above, this paper firstly develops a moving-window based two-stage forecasting framework. At the first stage, we propose four forecasting models using CNN and LSTM networks to learn the features of the data with different input and output

structures, namely single-input-single-output (SISO) model, multiple-input-single-output (MISO) model, single-input-multiple-output (SIMO) model and multiple-input-multiple-output (MIMO) model. After that, we conduct an experiment to explore which structure is more beneficial in wind power forecasting. At the second stage, we integrate the results from the first stage with RR method and use a moving-window algorithm to update the parameters of the ensemble model. Moreover, several statistical modeling methods are selected as benchmarks to demonstrate the advantage of RR in addressing the extrapolation error of the model. Finally, the forecasting results are compared with those generated by several existing algorithms.

In the following, Section 2 introduces the first-stage models; Section 3 describes the two-stage forecasting framework; Section 4 displays the experiment results, and Section 5 presents the concluding remarks.

2. Development of the first-stage models

The combination of CNN and LSTM has been widely used in the literature, e.g., Wu et al. [19] and Liu et al. [20], to develop a deep neural network for the wind power forecasting. In this study, we also make use of such a technique combination to build the SISO, SIMO, MISO and MIMO models at the first stage, respectively.

2.1. SISO model

The SISO model, as shown in Fig. 1, follows the structure that is extensively used in the literature, in which the input data are combined to enter in the forecasting model together and then output the single forecasting result.

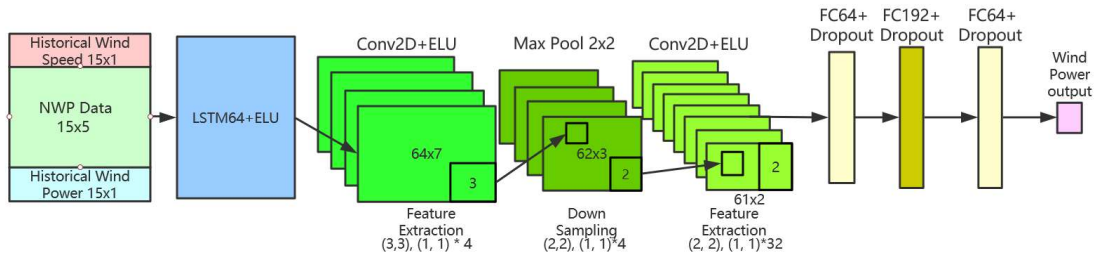


Figure 1. Architecture of SISO model using deep neural networks.

Given the prediction horizon h and time steps n , if we are at time t , we use the historical wind power data $x_p = \{\varphi_{p_{t-n}}, \dots, \varphi_{p_{t-1}}, \varphi_{p_t}\}$, historical wind speed data $x_s =$

$\{\varphi_{s_{t-n}}, \dots, \varphi_{s_{t-1}}, \varphi_{s_t}\}$, and NWP data $x_w = \{\varphi_{w_{t-h+1}}, \dots, \varphi_{w_{t+h}}, \varphi_{w_{t+h+1}}, \dots, \varphi_{w_{t+2h-1}}\}$ as input to build the forecasting model. As noted, the NWP data used in this study are obtained one day in advance; therefore, such settings are reasonable. The strategy of SISO model is to solve the regression problem by minimizing the loss function in every batch of output:

$$L_p = \frac{1}{m} \left(\sum ||\hat{\varphi}_{p_{t+h}} - \varphi_{p_{t+h}}||^2 \right), \quad (1)$$

where $\hat{\varphi}_{p_{t+h}}$ is the forecasting wind power results using the SISO model at time $t + h$, $\varphi_{p_{t+h}}$ is the actual wind power generation at time $t + h$ and m is the number of the total points used for modeling. As seen in Fig. 1, historical wind speed, historical wind power and NWP data are combined as a 15×7 matrix. 7 represents 7 input variables, namely five NWP variables (wind speed, wind direction, humidity, air pressure and temperature) and historical wind speed variable and historical wind power variable. If we are at 8 o'clock in the morning, for NWP data, 15 represents the data from 8:15 a.m. to 11:45 a.m.; for wind speed and power data, 15 represents the data from 4:30 a.m. to 8:00 a.m. The constructed matrix is accepted by a 64 hidden-size LSTM layer; after that, with the ELU activation function in the first layer, the outputs are passed to the CNN layers. Taking the first convolutional layer as an example, 64×7 represents the input size, 4 is the number of the kernels, (3, 3) indicates the kernel size, and (1, 1) is the step length. After three fully-connected (FC) layers, wind power is output at the last FC layer.

2.2. SIMO model

In the following, we present the architecture of the SIMO model. Compared to SISO model, SIMO model also forecasts wind speed besides forecasting wind power as shown in Fig. 2. The main idea behind SIMO model follows the structure of multiple-output learning. Hence, the loss function could be written as:

$$L_{p,s} = \frac{1}{m} \left(\alpha \sum ||\hat{\varphi}_{p_{t+h}} - \varphi_{p_{t+h}}||^2 \right) + \frac{1}{m} \left(\beta \sum ||\hat{\varphi}_{s_{t+h}} - \varphi_{s_{t+h}}||^2 \right), \quad (2)$$

where $\hat{\varphi}_{s_{t+h}}$ is the forecasting wind speed results at time $t + h$, $\varphi_{s_{t+h}}$ is the actual wind speed at time $t + h$, α and β are the weight parameters. The Pearson correlation coefficient

between real wind speed and wind power is greater than 0.933 in these three wind farms; hence, we set α and β as 1 and 0.9 in this study.

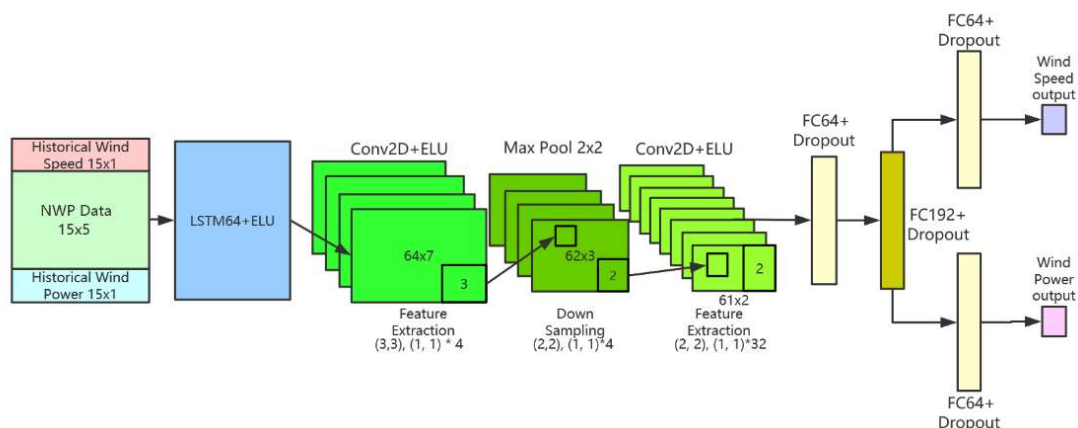


Figure 2. Architecture of SIMO model using deep neural networks.

2.3. MISO model

Taking NWP wind speed, real wind speed and wind power data in the same periods as shown in Fig. 3, we can find out that these three variables have high similarities to each other; however, NWP wind speed has smaller variances than the others, and NWP wind speed has less correlations with real wind power than real wind speed. Hence, the aim of the multiple-input structure is to explore whether learning different types of data separately is able to improve the forecasting accuracy or not, compared to SISO structure. Fig. 4 presents the architecture of the MISO model. As seen, to extract the features of NWP data, we still use SISO structure; however, for the historical wind speed and wind power data, we use another LSTM layers to learn their internal patterns, respectively. Before output, the extracted features from three different types of input data are concatenated.

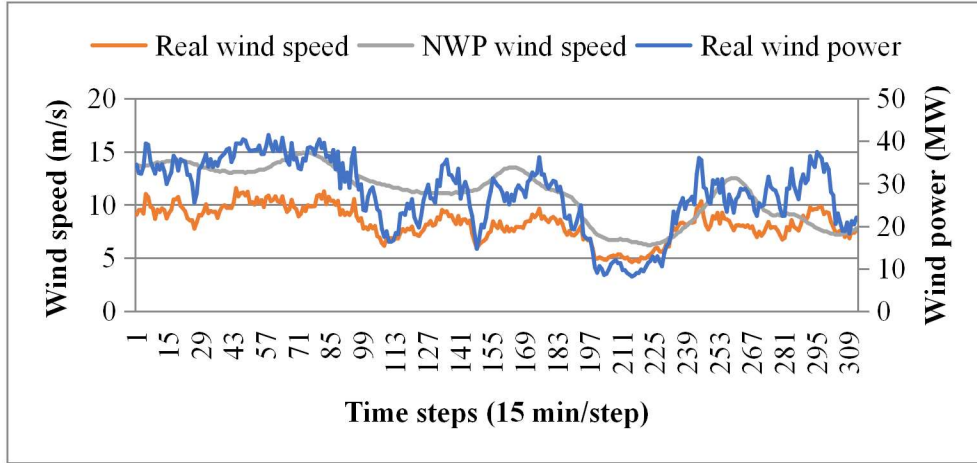


Figure 3. An example of NWP wind speed, real wind power and wind speed in the same

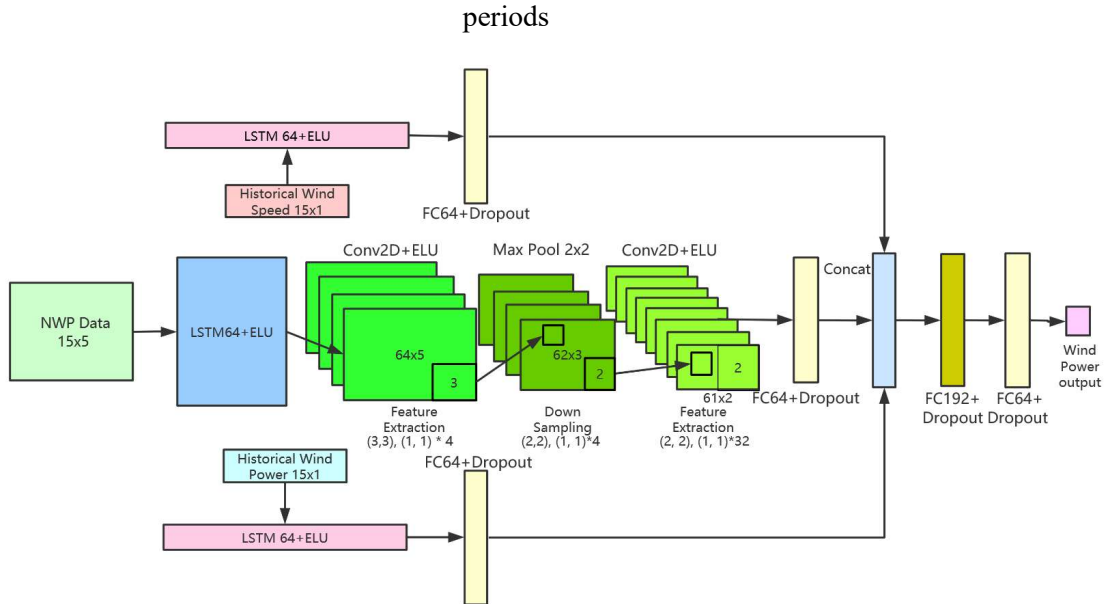


Figure 4. Architecture of MISO model using deep neural networks

2.4. MIMO model

The structure of the networks for MIMO model is an integration of MISO and SIMO models, as shown in Fig. 5. Compared to the other three, the architecture of MIMO model is the most complicated one; however, it should be noted that this does not guarantee it will produce the most accurate forecasting results than the others. When designing these four structures, we would like to investigate how the models perform when only changing the way of input-and-output structure. If the results of these four models have no significant differences to each other, the ensemble procedure has little meaning; otherwise, combining the forecasting results with a statistical method provides more potentials to further improve

the forecasting accuracy.

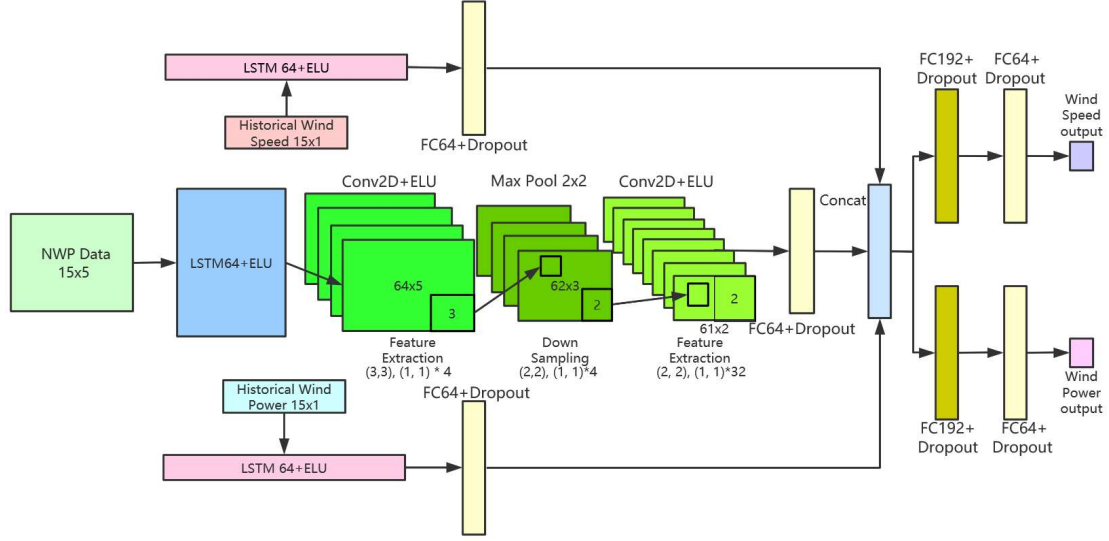


Figure 5. Architecture of MIMO model using deep neural networks

3. Two-stage forecasting framework

To develop a two-stage forecasting framework, the data used for each stage is critical. In this study, considering the over-fitting issue, we require first-stage and second-stage training sets have no crossover. In addition, we use a validation set to examine the goodness of the first-stage models. When forecasting wind power ramp events, a common assumption that the forecasting model does not depend on the long-term historical data is made [32]. Therefore, we exploit the latest data before the forecasting day as the validation set and second-stage training set for the further improvement of the forecasting accuracy. Note that the validation set might be the same as the second-stage training set or not.

Fig. 6 is the blueprint of the two-stage forecasting framework, which is built on the shelf of moving-window algorithm for the input data update. As shown in Fig. 6, there are two moving-window processes. Moving-window 1 is to move the training and testing datasets forward in a certain time period. Testing datasets are divided into daily subsets; therefore, Moving-window 2 is to move the second-stage training set forward as the testing subset evolves. In this study, we set the window size of the first-stage training set as one-year data. In addition, the window sizes of validation set, second-stage training set and testing set are all 10-day data. For example, if we would like to forecast the short-term wind power at Jan 11, 2020, we use the data at year 2019 as the first-stage data and the data from Jan 1 to Jan 10,

2020 as the validation set and second-stage training set. When forecasting the wind power at Jan 20, 2020, we still use the data at year 2019 as the first-stage data but the second-stage data are updated to Jan 10 to Jan 19, 2020. Subsequently, for the forecasting at Jan 21, 2020, we will make use of the data from Jan 11, 2019 to Jan 10, 2020 to train the models at the first stage, and utilize the data from Jan 11 to Jan 20, 2020 as the validation set and second-stage training set.

Besides the moving-window algorithms, at the first stage, the four proposed deep neural networks in Section 2 are applied to the first-stage data to train the models. At the second stage, the first-stage models (MIMO, MISO, SIMO and SISO) are applied to the second-stage training set to obtain the forecasting results $\hat{Y}_\alpha, \hat{Y}_\beta, \hat{Y}_\gamma$ and \hat{Y}_δ , respectively. These forecasting results and their corresponding real power, Y_{t2} , are used to generate a new dataset for training the ensemble model using RR method. When forecasting the next-period wind power, the testing data will be firstly entered into the four well trained models at the first stage to achieve $\hat{Y}'_\alpha, \hat{Y}'_\beta, \hat{Y}'_\gamma$ and \hat{Y}'_δ , which will then be entered into the RR model through the “blue lines” shown in Fig. 6. The detailed information about this two-stage forecasting framework is presented in Algorithm 1.

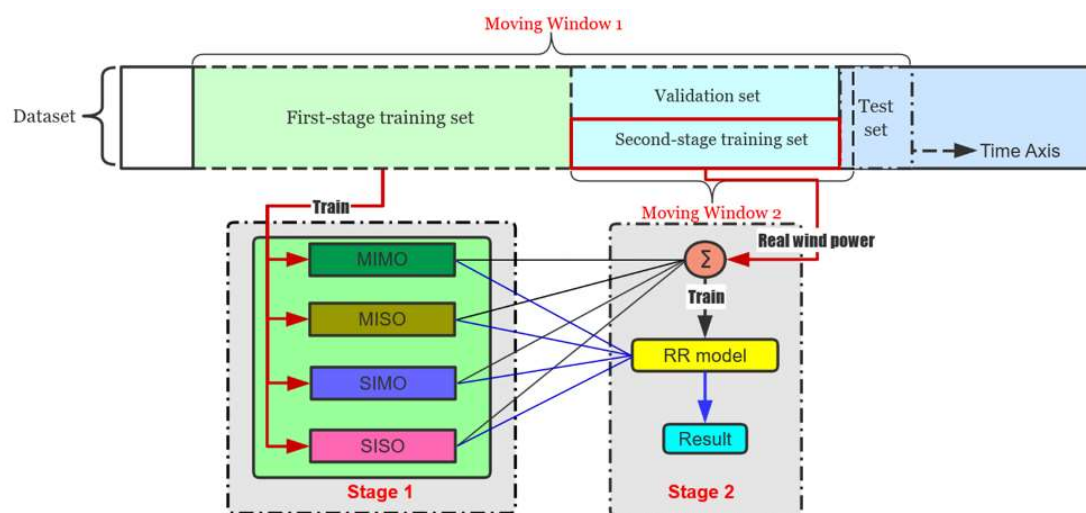


Figure 6. Two-stage forecasting framework proposed in this study

Algorithm 1 Two-stage forecasting algorithm proposed in this study

Require:

S_{t1} : First stage training set .

S_{t2} : Second stage training set.

S_{v1} :First stage validation set.
 S_{te} :Test set.
 t_1 :Starting point of S_{t1} .
 t_2 :Starting point of S_{t2} .
 t_v :Starting point of S_{v1} .
 t_e :Starting point of S_{te} .
 l_{c1} :Stage 1 update cycle, which is defined as an integral multiple of l_{c2} .
 l_{c2} :Stage 2 update cycle.
 X_{t1} :input data of S_{t1} .
 X_{t2} :input data of S_{t2} .
 X_{v1} :input data of S_{v1} .
 X_{te} :input data of S_{te} .
 Y_{t1} :Real power observation of S_{t1} .
 Y_{t2} :Real power observation of S_{t2} .
 Y_{v1} :Real power observation of S_{v1} .
 M_α :MIMO model with output \hat{Y}_α .
 M_β :MISO model with output \hat{Y}_β .
 M_γ :SIMO model with output \hat{Y}_γ .
 M_δ :SISO model with output \hat{Y}_δ .
 M_{RR} :RR model with output \hat{Y} .
1:while S_{te} is not null:
 2:do train $M_\alpha, M_\beta, M_\gamma, M_\delta$ with input X_{t1} and output Y_{t1} as training set,
 and validate them with input X_{v1} and output Y_{v1} .
 3:for $i \leftarrow 1$ to $(\frac{l_{c1}}{l_{c2}})$:
 4:do collect $\hat{Y}_\alpha \leftarrow M_\alpha(X_{t2}), \hat{Y}_\beta \leftarrow M_\beta(X_{t2}), \hat{Y}_\gamma \leftarrow M_\gamma(X_{t2}), \hat{Y}_\delta \leftarrow M_\delta(X_{t2})$
 5: train M_{LR} with $\hat{Y}_\alpha, \hat{Y}_\beta, \hat{Y}_\gamma, \hat{Y}_\delta$ as input and Y_{t2} as output
 6:for $j \leftarrow 1$ to l_{c2} :
 7:do collect $\hat{Y}_\alpha[j] \leftarrow M_\alpha(X_{te}[j]), \hat{Y}_\beta[j] \leftarrow M_\beta(X_{te}[j]),$
 $\hat{Y}_\gamma[j] \leftarrow M_\gamma(X_{te}[j]), \hat{Y}_\delta[j] \leftarrow M_\delta(X_{te}[j])$
 8:get RESULT: $\hat{Y}_{te}[j] \leftarrow M_{LR}(\hat{Y}_\alpha[j], \hat{Y}_\beta[j], \hat{Y}_\gamma[j], \hat{Y}_\delta[j])$
 9: $t_v \leftarrow t_v + l_{c2}, t_e \leftarrow t_e + l_{c2}$
 10:update S_{t2}, S_{te}
 11: $t_1 \leftarrow t_1 + l_{c1}$
 12: $t_2 \leftarrow t_2 + l_{c1}$
 13:update S_{t1}, S_{t2}
14:end while

4. Case study

4.1. Wind-farm data description

In this study, we implement our model at three wind farms in the Fujian Province of China to evaluate short-term WPF accuracy. The basic information of these wind farms is shown in Table 1. As observed, the wind conditions of these three wind farms are not quite the same by observing the mean and standard deviations of wind speed and wind power of these three wind farms, which denotes the experiment results can show the generalization of the forecasting models.

The data obtained cover 2018–2019. We randomly select 10-day data from each season as testing set to examine the performance of the developed models. Hence, when moving-window 1 moves to the new step, for the first day forecasting, evaluation set coincides with second-stage training set.

Table 1. Basic information of wind farms used in this study

No. of wind farm (WF)	WF 1	WF 2	WF 3
Number of wind turbines	33	24	24
Installed capacity	49.5 MW	48 MW	48 MW
Type of manufacturer	Envision EN70-1500	Vestas V80-2000	Gamesa G90
Hub-height of the tower(s)	70 m	80 m	90 m
Cut-in/cut-out wind speed	4.0 m/s / 25 m/s	3.5 m/s / 25 m/s	3 m/s / 21 m/s
Rated wind speed	11.6 m/s	14.5 m/s	11 m/s
Swept area	3915 m ²	5027 m ²	6362 m ²
Mean wind speed	5.38 m/s	5.73 m/s	6.25 m/s
Mean wind power	12.73 MW	12.91 MW	12.07 MW
Standard deviation of wind speed	2.85	3.33	3.53
Standard deviation of wind power	12.89	12.87	13.51

4.2. Forecasting results

In this section, we implement the proposed model to forecast the 2-h ahead wind power at the three given wind farms. Following the literature, we use the root mean-square error (RMSE) and mean absolute error (MAE) to evaluate the performance of the forecasting results.

$$RMSE = \sqrt{\frac{1}{N} \sum_{i=1}^N (P_i^r - P_i^f)^2} \quad , \quad (3)$$

$$MAE = \frac{1}{N} \sum_{i=1}^N |P_i^r - P_i^f| \quad , \quad (4)$$

where N is the total forecasting points. P^r is the real wind-power generation and P^f is the forecasting wind-power generation.

4.2.1. Experiment 1

In the first experiment, considering the different structures of the models at the first stage, we investigate how the four models presented in Section 2 perform in the forecasting accuracy. Note that in this experiment, there is no moving-window 2 procedure as presented in Fig. 6. In other words, we build the first-stage models and then use them to forecast 10-day wind power in order to examine the performance of these four models. We use WF1, WF2, WF3 to represent wind farm 1, wind farm 2, and wind farm 3, respectively. After using the evaluation measurement presented in Eqs. (3) and (4), we have the results of four seasons shown in Table 2.

As seen, for each season, the accuracies of the proposed models are different; however, most of the results from SIMO model have the best forecasting accuracies. To better show the general performance of these four models, we average the forecasting accuracy of four seasons and present them in Fig. 7.

Table 2. Forecasting results comparison between presented four models in each season

Spring						Summer					
		MIMO	MISO	SIMO	SISO			MIMO	MISO	SIMO	SISO
WF1	RMSE	5.5242	5.5795	5.3376	5.7981	WF1	RMSE	3.6307	3.7707	3.5861	3.8215
	MAE	4.2093	4.2734	4.0671	4.4994		MAE	2.0724	2.2217	2.0469	2.3701
WF2	RMSE	2.9125	2.925	2.5205	2.704	WF2	RMSE	4.3182	4.3391	4.0855	4.5418
	MAE	1.8784	1.8315	1.6091	1.7583		MAE	3.2826	3.3305	3.1694	3.5356
WF3	RMSE	2.3081	2.2459	2.0235	2.2106	WF3	RMSE	5.4227	5.567	4.7035	5.1366
	MAE	1.3194	1.4657	1.1654	1.4309		MAE	4.0186	4.1316	3.5202	3.8857
Autumn						Winter					
		MIMO	MISO	SIMO	SISO			MIMO	MISO	SIMO	SISO
WF1	RMSE	5.2346	5.2490	4.9586	5.0682	WF1	RMSE	5.0679	5.2256	4.8618	5.1487
	MAE	3.8446	3.8977	3.6221	3.8527		MAE	3.5209	3.73	3.3299	3.6106
WF2	RMSE	4.0866	4.1866	3.8224	4.0557	WF2	RMSE	4.7144	4.7109	4.7249	4.8591
	MAE	2.9126	3.0005	2.7651	2.9071		MAE	3.3419	3.3122	3.3112	3.5154
WF3	RMSE	5.2954	5.2845	4.5240	4.6975	WF3	RMSE	4.9402	5.0171	4.9409	5.1371
	MAE	3.5466	3.4424	2.9324	3.1839		MAE	3.7694	3.8224	3.8051	3.9060

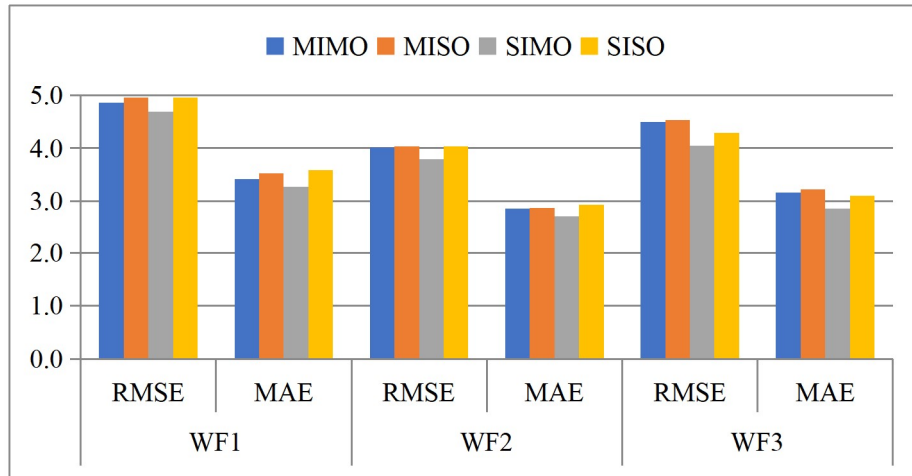


Figure 7. Average forecasting accuracy comparison of the four proposed forecasting models.

In Fig. 7, all the results from the three wind farms have the best forecasting accuracy using SIMO model, compared to the others. Further, as noted, MIMO model has a slightly better performance than MISO model in these three cases, which means the multiple-output structure is a way to improve the forecasting accuracy. However, comparing MISO to SISO, we cannot obtain the clear conclusion that the multiple-input structure can improve the forecasting accuracy. Hence, for this specific study, such results indicate when learning the features of the data, it is better to mix them together as a single input; moreover, adding an auxiliary output can help improve the forecasting accuracy. In addition, we illustrate the variances of the absolute difference between predicted wind power and real wind power from the four proposed models in Fig. 8. As observed, the difference variances are not quite the same to each other in each case; however, the variances of SIMO model have the lowest one in all cases, which implies SIMO model generates the more consistently stable results than the others.

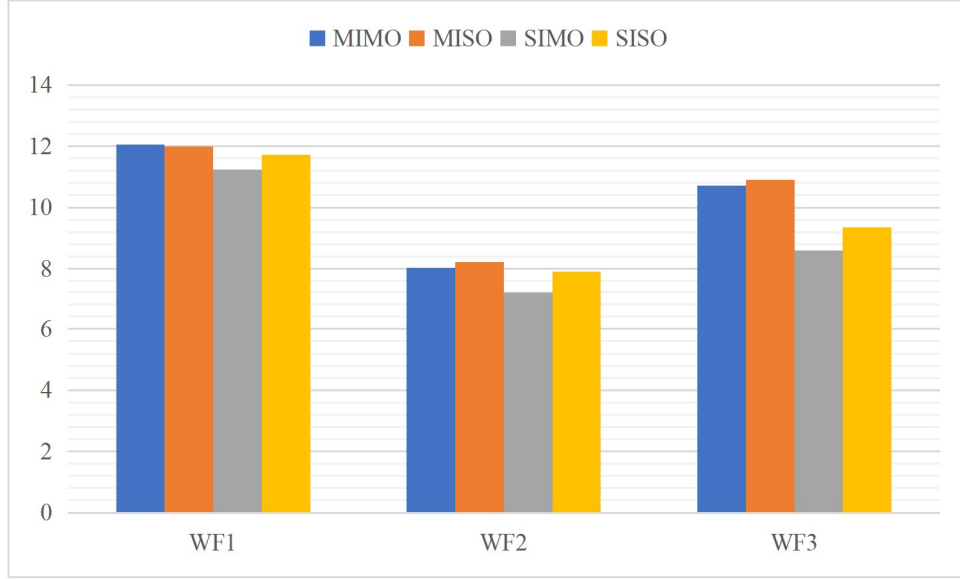


Figure 8. Variances of the absolute difference between predicted wind power and real wind power from four proposed models.

4.2.2. Experiment 2

In this section, we implement the proposed two-stage framework to build the forecasting model. Even though the SIMO model in Section 4.2.1 has shown distinguished performance compared to the others, the second stage of the framework aims to further improve the accuracy with the application of RR model. As aforementioned, we prefer to use the latest information before the forecasting day to build the ensemble model. Even though this method would update the ensemble model in time effectively, it may also lead to the model extrapolation due to the quantity of the input data. Hence, the selection of the modeling technique at the second stage becomes paramount. To better demonstrate the performance of RR method, we also exploit support vector regression (SVR), artificial neural networks (ANN) and Gaussian process regression (GPR) methods as benchmarks.

The forecasting accuracies of each season using different statistical modeling techniques are presented in Table 3. As seen, not every ensemble model has a better performance than SIMO model in all cases; however, RR model outperforms SIMO model in each case. More importantly, it is found out that machine learning techniques do not show the outstanding performance for the second-stage model, compared to RR method. Especially, in some cases, SVR and GPR based ensemble models have much worse performance than the others, which are marked as red in Table 3. To investigate this, we plot the forecasting results

of WF3 winter case in Fig. 9.

Table 3. Forecasting accuracy comparison using different modeling techniques for ensemble

	Spring	SIMO	RR	SVR	ANN	GPR		Summer	SIMO	RR	SVR	ANN	GPR
WF1	RMSE	5.3376	5.2612	5.4061	5.2697	5.4689	WF1	RMSE	3.5861	3.4939	3.4281	3.5430	3.4691
	MAE	4.0671	4.0077	4.0857	3.9931	4.2199		MAE	2.0469	1.9085	1.8168	2.0917	1.9829
WF2	RMSE	2.5205	2.4865	2.4887	2.5469	2.5748	WF2	RMSE	4.0855	3.9674	4.0611	3.9793	4.1710
	MAE	1.6091	1.5803	1.4260	1.5800	1.5519		MAE	3.1694	3.0383	3.1411	3.0375	3.1980
WF3	RMSE	2.0235	2.0183	2.0561	2.1224	2.1118	WF3	RMSE	4.7035	4.6511	4.5685	4.7544	4.6760
	MAE	1.1654	1.1502	1.0217	1.1678	1.1285		MAE	3.5202	3.4728	3.3738	3.5205	3.4811
	Autumn	SIMO	RR	SVR	ANN	GPR		Winter	SIMO	RR	SVR	ANN	GPR
WF1	RMSE	4.9586	4.7464	4.8681	4.8041	4.8259	WF1	RMSE	4.8618	4.7531	4.8418	4.6949	5.2367
	MAE	3.6221	3.5090	3.5100	3.6443	3.5612		MAE	3.3299	3.2343	3.2055	3.1636	3.6595
WF2	RMSE	3.8224	3.6748	4.2732	3.8029	5.1703	WF2	RMSE	4.7249	4.5551	4.8481	4.6041	5.1104
	MAE	2.7651	2.6277	2.9386	2.7373	3.3129		MAE	3.3112	3.2276	3.3947	3.2898	3.7321
WF3	RMSE	4.524	4.3834	4.5486	4.4422	5.3223	WF3	RMSE	4.9409	4.6874	6.2021	4.9197	7.6411
	MAE	2.9324	2.8778	2.9795	2.9548	3.3843		MAE	3.8051	3.5662	4.3800	3.7487	4.9461

As observed in Fig. 9, all four forecasting methods have similar performance except in the steps 729-785, SVR and GPR based ensemble models lead to very different forecasting results (marked with a red circle) than the others. Such irrational forecasting phenomenon occurs in eighth forecasting day. Hence, we explore the input information that builds the eighth ensemble model and the input information for examining the eighth model in Fig. 10, where the first 1000 data are for ensemble model construction and the rest are for testing. As seen, when building the ensemble model, the range of the input data is between 0 and 38 MW; however, the rest data have some over 38 MW (see the dashed rectangle in Fig. 10). In this specific case, SVR and GPR based models may be very sensitive to the extrapolation issue so that the forecasting results become much worse in the testing day 8. As a comparison, RR and

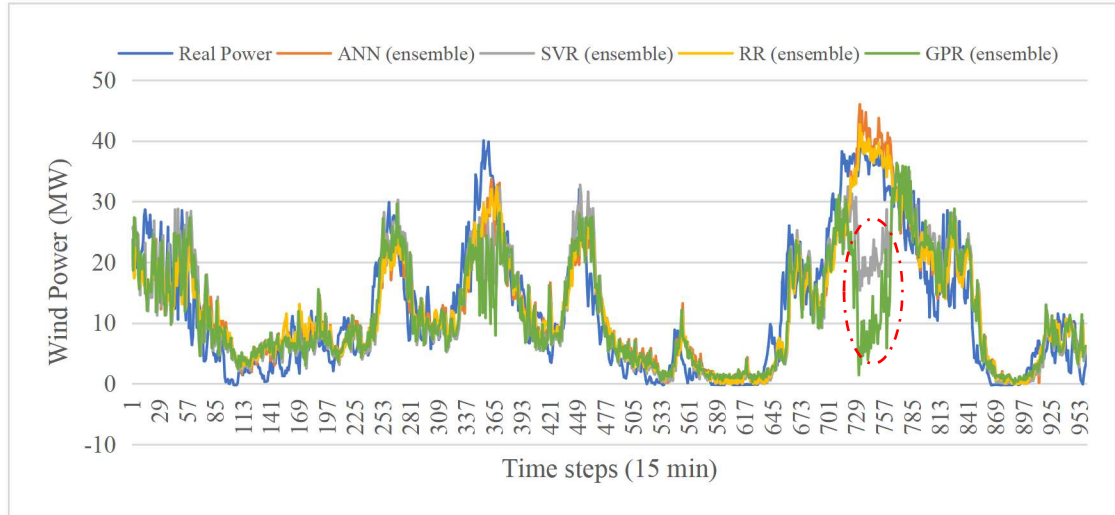


Figure 9. Ten-day forecasting results in the winter case of WF3 using different ensemble techniques

ANN methods have a good performance when the extrapolation of the model occurs. Such experiments not only demonstrate the advantage of RR as an ensemble modeling technique but also denote the importance of the modeling technique selection considering the extrapolation issue.

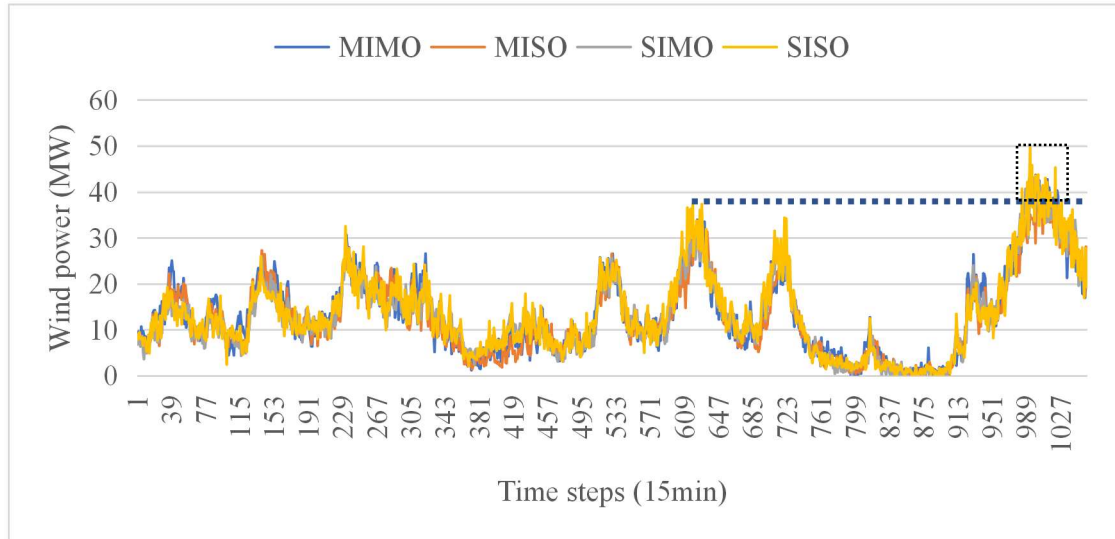


Figure 10. Input information illustration for the eighth day forecasting in the winter case of WF3 (the first 1000 data are for modeling and the rest are for testing).

4.2.3. Experiment 3

In this section, we exploit four existing methods as benchmarks to demonstrate the performance of the proposed forecasting algorithm. Specifically, we exploit persistence model (P) and ARIMA model, which have been widely used in the literature as benchmarks for the

short-term wind power/speed forecasting. In addition, we utilize the SVR based forecasting model (SVR_f) from Sarikprueck et al. [33] as another benchmark. Lastly, we remove the LSTM and convolutional layers in SIMO model to build a new forecasting model with only FC layers, which is regarded as using traditional artificial neural networks (ANN_f) to construct the forecasting model. The forecasting accuracy results are presented in Table 4. As seen, in most cases, the proposed two-stage forecasting (TSF) algorithm performs better than the existing ones. Even though sometimes, SVR_f method has a slightly better performance than the TSF method in terms of MAE, this method also results in the worse forecasting accuracy in the other cases. For the further investigation between the TSF and SVR_f algorithms, we plot the 10-day forecasting results in the Spring case of WF1. As shown in Fig. 11, the proposed algorithm seems to generate the closer forecasting results to the real wind power than SVR_f method, especially inside the black circle. Moreover, we integrate all the forecasting results together and statistically analyze the absolute difference between forecasting results and the real wind power. As shown in Table 5, the TSF algorithm leads to the lowest mean and variance, which indicates the proposed algorithm is able to generate more accurate and stable results than the other methods. Even though the mean of SVR_f method is slightly worse than that of the TSF algorithm, its variance is much bigger, which connotes the SVR_f method may generate the less stable results than the TSF algorithm.

Table 4. Forecasting accuracy comparison between the proposed two-stage forecasting (TSF) algorithm and the existing ones

	Spring	TSF	P	SVR _f	ANN _f	ARIMA		Summer	TSF	P	SVR _f	ANN _f	ARIMA
WF1	RMSE	5.2612	5.9184	5.3201	5.5617	6.1944	WF1	RMSE	3.4939	4.0955	3.7485	3.9543	4.4910
	MAE	4.0377	4.3259	3.8785	4.1690	4.6378		MAE	1.9085	2.0696	1.9627	2.1562	2.2277
WF2	RMSE	2.4865	2.8930	2.4891	2.7396	2.9794	WF2	RMSE	3.9674	4.4904	4.2450	4.1354	4.6609
	MAE	1.5803	1.6245	1.5935	1.6951	1.6854		MAE	3.0383	3.3055	3.2568	3.2249	3.4266
WF3	RMSE	2.0483	2.3462	2.2469	2.979	2.4515	WF3	RMSE	4.6511	5.9998	5.5993	5.2180	6.3524
	MAE	1.1502	1.2481	1.0412	2.2115	1.2827		MAE	3.4728	4.2760	3.9678	3.9425	4.6812
	Autumn	TSF	P	SVR _f	ANN _f	ARIMA		Winter	TSF	P	SVR _f	ANN _f	ARIMA
WF1	RMSE	4.7464	5.5783	5.5869	5.9684	5.9430	WF1	RMSE	4.7531	5.4044	5.1818	5.0692	5.6672
	MAE	3.5090	3.8938	3.9398	4.2516	4.3409		MAE	3.2343	3.5594	3.3073	3.3917	3.9695
WF2	RMSE	3.6748	4.4854	4.1025	4.1008	4.6135	WF2	RMSE	4.5551	4.8692	4.8692	4.9768	5.1203
	MAE	2.6277	3.2049	2.8699	2.9030	3.3434		MAE	3.1276	3.2013	3.2013	3.4768	3.5799
WF3	RMSE	4.3834	6.296	5.9204	5.5003	6.7510	WF3	RMSE	4.6874	5.2915	5.4555	6.9488	5.3920

Table 5. Absolute difference analysis between the real wind power (WP) and forecasting results

	TSF vs WP	P vs WP	SVR _f vs WP	ANN _f vs WP	ARIMA vs WP
Variance	8.5034	13.1778	11.9421	11.7409	13.8744
Mean	2.6487	2.9593	2.7801	3.0991	3.2395

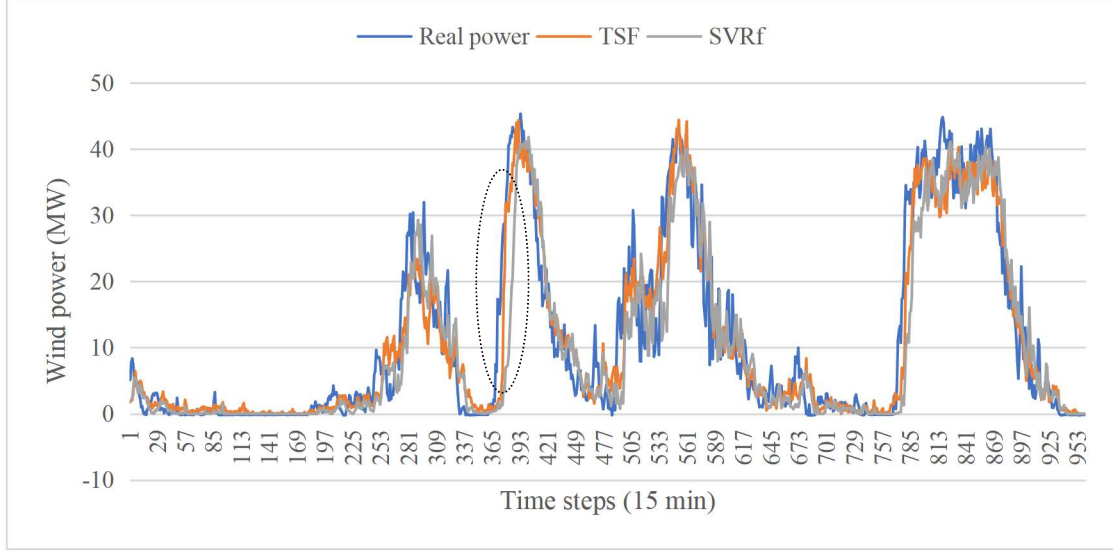


Figure 11. An example of forecasting results using proposed algorithm and SVR_f method.

5. Conclusion

WPF using ensemble model is a widely studied topic. Compared to the literature works, this paper makes use of the day-ahead NWP data and historical wind data as input to develop a two-stage forecasting framework on the shelf of moving window algorithm. Specifically, we propose four models with deep neural networks at the first stage. The four models use the same parameters in the CNN and LSTM layers except their input and output structures. Experiment 1 demonstrates that SIMO model results in better forecasting accuracies than the other three, which indicates the multiple-output learning structure is a way for the improvement of the forecasting accuracy in the wind power field; however, the multiple-input learning structure cannot bring any benefits in this study. Moreover, after using the proposed TSF algorithm to forecast the wind power generations, we find out that the TSF algorithm using RR method is able to further improve the forecasting accuracy as shown in Table 4, compared to SIMO model in all cases. More importantly, as Figs. 8 and 9 illustrated, some

machine learning techniques are likely to lead to the extrapolation errors, which denotes the importance of selecting the ensemble model. In the end, we compare the proposed TSF algorithm with several existing algorithms. Even though SVR_f method sometimes leads to a better accuracy in terms of MAE, this method has bigger RMSE values in all cases, and also has bigger absolute mean and variance difference than TSF algorithm as shown in Tables 4 and 5. All in all, the proposed TSF algorithm is able to generate more accurate and stable forecasting results than the existing ones.

Acknowledgments

This study was supported by the National Natural Science Foundation of China (Grant No. 91846301) and Postdoctoral funding of Heilongjiang Province (Grant No. LBH-Z19146)

Conflict of Interests

The authors declare no conflicts of interest.

References

- [1] Sahu BK, Hiloidhari M, Baruah D. Global trend in wind power with special focus on the top five wind power producing countries. *Renewable Sustainable Energy Reviews*, 2013;19:348–359.
- [2] Xinyu Z, Jinfu L, Daren Y, Juntao C. One-day-ahead probabilistic wind speed forecast based on optimized numerical weather prediction data. *Energy Conversion and Management*, 2018;164:560–569.
- [3] Wang J, Botterud A, Bessa R, Keko H, Carvalho L, Issicaba D, Sumaili J, Miranda V. Wind power forecasting uncertainty and unit commitment. *Applied Energy*, 2011; 88(11):4014-4023.
- [4] Mendes J, Sumaili J, Bessa R, Keko H, Miranda V, Botterud A, Zhou Z. Very short-term wind power forecasting: state-of-the-art. Technical report, Argonne National Laboratory (ANL); 2013.
- [5] Al-Yahyai S, Charabi Y, Gastli A. Review of the use of numerical weather prediction (NWP) models for wind energy assessment. *Renewable Sustainable Energy Reviews*, 2010;14(9):3192-3198.
- [6] Black T. The new NMC mesoscale Eta model description and forecasting examples. *American Meteorological Society AMS*, 1994;9:265-278.

- [7] Chou SC, Tanajura CAS, Xue Y, Nobre CA. Validation of the coupled Eta/SSiB model over South America. *Journal of Geophysical Research*, 2002, 107, LBA56-1–LBA56-20.
- [8] Grell GA, Dudhia J, Stauffer DR. A description of the fifth-generation Penn State/NCAR mesoscale model (MM5). National Center for Atmospheric Research. Boulder: s.n., Technical Report. NCAR/TN-398+STR,1994.
- [9] NCAR. MM5 model website. <https://www2.mmm.ucar.edu/mm5/> accessed at Jan 9, 2020.
- [10] NCAR. WRF version 3 modeling system user's guide. Mesoscale & Microscale Meteorology Division, National Weather for Atmospheric Research NCAR. s.l.; 2008
- [11] UNCAR. WRF model: <http://www.mmm.ucar.edu/wrf/2009> accessed at Jan 9, 2020.
- [12] Erdem E , Shi J . ARMA based approaches for forecasting the tuple of wind speed and direction[J]. *Applied Energy*, 2011, 88(4):1405-1414.
- [13] Zhang Y, Zhao Y, Kong C, Chen B. A new prediction method based on VMD-PRBF-ARMA-E model considering wind speed characteristic. *Energy Conversion and Management*, 2020;203:112254.
- [14] Cadenas E, Rivera W, Campos-Amezcuca R, Heard C. Wind speed prediction using a univariate ARIMA model and a multivariate NARX model. *Energies*, 2016;9:109.
- [15] Cassola F, Burlando M. Wind speed and wind energy forecast through Kalman filtering of Numerical Weather Prediction model output. *Applied Energy*, 2012;99:154–166.
- [16] Li Y, Wu H, Liu H. Multi-step wind speed forecasting using EWT decomposition, LSTM principal computing, RELM subordinate computing and IEWT reconstruction. *Energy Conversion and Management*, 2018;167:203–219.
- [17] Ya-Lan H, Liang C. A nonlinear hybrid wind speed forecasting model using LSTM network, hysteretic ELM and Differential Evolution algorithm. *Energy Conversion and Management*, 2018;173:123–142.
- [18] Ruiguo Y, Jie G, Mei Y, Wenhuan L, Tianyi X, Mankun Z, Jie Z, Ruixuan Z, Zhuo Z. LSTM-EFG for wind power forecasting based on sequential correlation features. *Future Generation Computer Systems*, 2019;93:33–42.
- [19] Wu W, Chen K, Qiao Y, Lu Z. Probabilistic short-term wind power forecasting based on deep neural networks. 2016 International Conference on Probabilistic Methods Applied to Power System (PMAPS), Beijing, 16-20 Oct. 2016.

- [20] Liu H, Mi X, Li Y. Smart deep learning based wind speed prediction model using wavelet packet decomposition convolutional neural network and convolutional long short term memory network. *Energy Conversion and Management*, 2018;166:120–131.
- [21] Freedman JM, Manobianco J, Schroeder J, Ancell B, Brewster K, Basu S, et al. The wind forecast improvement project (WFIP): a public/private partnership for improving short term wind energy forecasts and quantifying the benefits of utility operations. the southern study area, final report. Tech. rep.; Apr 2014
- [22] Feng C, Cui M, Hodge B, Zhang J. A data-driven multi-model methodology with deep feature selection for short-term wind forecasting. *Applied Energy* 190:1245–1257.
- [23] Wang H, Li G, Wang G, Peng J, Jiang H, Liu Y. (2017) Deep learning based ensemble approach for probabilistic wind power forecasting. *Applied Energy*, 188: 56-70.
- [24] Hao Y, Tian C. A novel two-stage forecasting model based on error factor and ensemble method for multi-step wind power forecasting. *Applied Energy*, 238:368-383.
- [25] Liu H, Tian H, Chen C, Li Y. A hybrid statistical method to predict wind speed and wind power. *Renew Energy* 2010;35(8):1857–1861.
- [26] Liu H, Duan Z. (2020) Corrected multi-resolution ensemble model for wind power forecasting with real-time decomposition and bivariate kernel density estimation. *Energy Conversion and Management*. 203: 112265.
- [27] Wang H, Lei Z, Liu Y, Peng J, Liu J. (2019) Echo state network based ensemble approach for wind power forecasting. *Energy Conversion and Management*, 201: 112188.
- [28] Xu D, Shi Y, Tsang IW, Ong Y. Gong C. Shen X (2019) A survey on multi-output learning. *arXiv*:1901.00248.
- [29] Jiejie Zhao, Bowen Du, Leilei Sun, Fuzhen Zhuang, Weifeng Lv, and Hui Xiong. 2019. Multiple Relational Attention Network for Multi-task Learning. In *Proceedings of the 25th ACM SIGKDD International Conference on Knowledge Discovery & Data Mining (KDD '19)*. Association for Computing Machinery, New York, NY, USA, 1123–1131.
- [30] Meisner BN (1979) Ridge regression-time extrapolation applied to Hawaiian rainfall normals. *Journal of Applied Meteorology*, 18(7): 904-912.
- [31] Kutner HK, Nachtsim CJ, Neter J, Li W. (2004) *Applied linear regression models*, Fifth Edition, McGraw-Hill, Irwin.

- [32] Dorado-Moreno M, Navarin N, Gutierrez PA, Prieto L, Sperduti A, Salcedo-Sanz S, Hervas-Martinez C. (2020) Multi-task learning for the prediction of wind power ramp events with deep neural networks. *Neural Networks*, 123, 401-411.
- [33] Sarikprueck P. Forecasting of wind, PV generation, and market price for the optimal operations of the regional PEV charging stations. Ph.D. dissertation, University of Texas at Arlington, 2015.